Easy Volcanic Aerosol version 2: progress toward an updated volcanic aerosol forcing generator

Sujan Khanal[1] (sujan.khanal@usask.ca), Matthew Toohey[1], Thomas Aubry[2], Domenic Neufeld[1]

[1]Institute of Space and Atmospheric Studies, University of Saskatchewan, Canada

[2]Department of Earth and Environmental Sciences, University of Exeter, UK

Introduction

- The Easy Volcanic Aerosol (EVA) family of simple models offers an approach to generate stratospheric aerosol fields from estimates of volcanic emissions.
- EVA takes as input a time series of volcanic eruption data, including the mass of sulfur injected into the stratosphere and location of the eruptions, and outputs aerosol optical properties as a function of time, latitude, height and wavelength based on a simple box-model of stratospheric transport.
- These aerosol properties are tailored for use as volcanic aerosol forcing in climate models. They are also useful as general quantitative estimates of the impact of volcanic eruptions on climate.
- EVA version 1 (Toohey et al., 2016) was based on observations of the aerosol from the 1991 Mt. Pinatubo eruption, while EVA_H (Aubry et al., 2020) was parameterized to improve agreement with a range of smaller magnitude eruptions observed over the 1979-2015 period, taking account of the estimated injection height of the emitted sulfur.
- Here, we present progress in the development of EVA version 2, which improves the fidelity of its output based on various important updates.

Box-model

Improved spatial structure with 5-box stratosphere

- EVA1 used a 3-box representation of the stratosphere, based on the "tropical pipe" conceptual model (Plumb et al., 1996). To better represent height dependency, EVA_H used an 8-box representation.
- For EVA2, we use a 5-box model, adding boxes for the lowermost stratosphere (LMS) of each hemisphere (Fig. 1).
- While maintaining a degree of simplicity, inclusion of separate boxes for the lowermost stratosphere of each hemisphere strongly improves agreement of vertical aerosol extinction with observations.

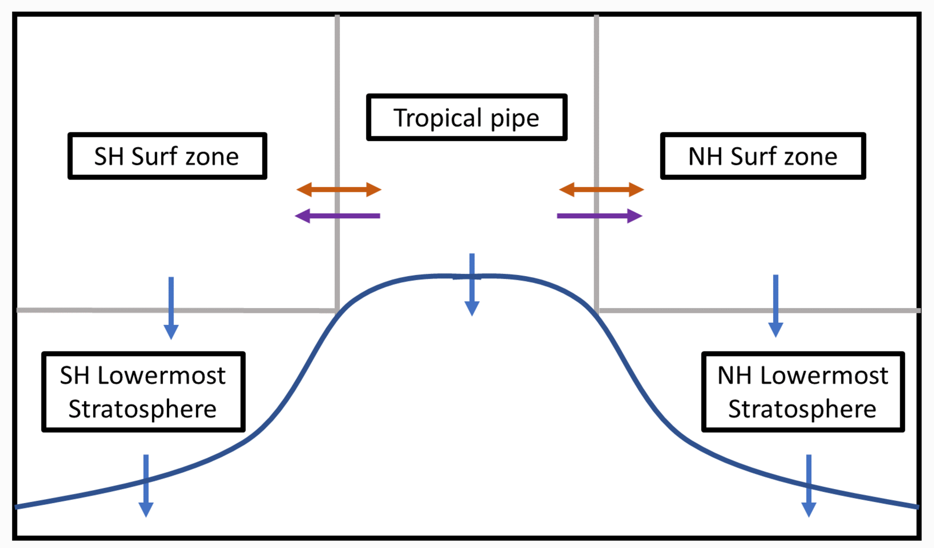

Figure 1: Schematic of EVA2 5-box representation of stratospheric aerosol mixing and removal. Arrows indicate (orange) two-way mixing, (purple) residual mass circulation and (blue) removal. Blue contour represents the tropopause.

Injection-height-dependent decay timescale

- Based on stratospheric aerosol residence time considerations, in EVA2, the stratospheric removal (decay) timescale is eruption specific and depends on the injection height and latitude. This allows the model to account for fast removal of aerosol from eruptions with injection heights close to the tropopause.
- The model makes use of the eruption parameters from the MSVOLSO2L4 volcanic emission database (Carn, 2022).
- Parameters specifying the vertical dependence of decay timescale in tropics and extratropics can be tuned to produce best fit with the Global Space-based Stratospheric Aerosol Climatology (GloSSAC, Kovilakam et al., 2020).

Stratospheric aerosol: refractive index and particle size distribution

Aerosol optical properties output by EVA at 550 nm are converted to other wavelengths using pre-computed lookup tables (LUTs) based on Mie scattering calculations with PyMieScatt (Sumlin et al., 2018).

Expanded and improved complex refractive index basis for calculations

- Compared to EVA1, EVA2 uses higher spectral resolution complex refractive indices (RI) of sulfuric acid-water solution to compute the lookup tables (LUTs). 10 refractive index datasets have been catalogued and this allows the model to account for different temperatures and sulfuric acid concentrations spanning nearly the entire range observed in stratosphere.
- LUT output includes aerosol extinction efficiency, single scattering albedo, and asymmetry parameter as a function of wavelength and effective radius.
- Imaginary part of the RI at longer wavelengths (> about 25μm) for Biermann et al., (2000) and Palmer and Williams (1975) data has been extrapolated using Hummel et al., (1988) data.

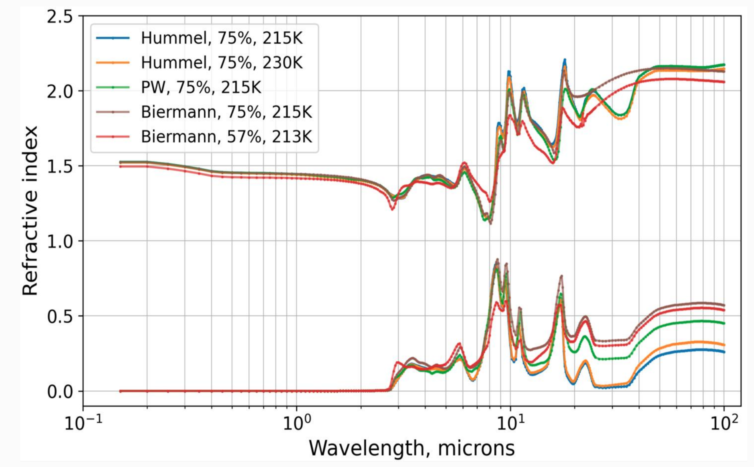

Figure 2: Complex RI of sulfuric acid-water solution for different datasets.

Improved particle size distributions based on observations

- EVA1 used a unimodal lognormal distribution with geometric standard deviation $S = 1.2$.
- EVA2 uses bimodal lognormal distribution, in line with in-situ observations of stratospheric aerosols from the Pinatubo eruption (Deshler et al., 1993), to estimate aerosol particle size distributions. Modes at smaller and larger radii have S of 1.8 and 1.25, respectively. The bimodal distribution is relevant for effective radii between roughly 0.4 and 0.75 μm, i.e., for bigger eruptions like El Chichón and Pinatubo.

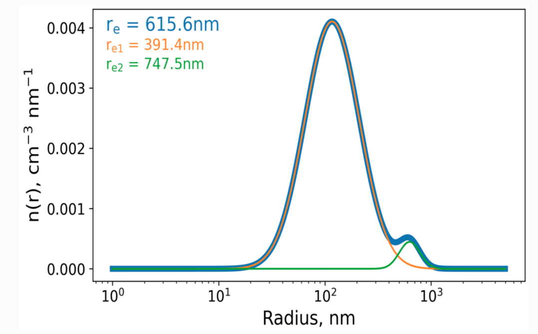

Figure 3: Bimodal particle size distribution example corresponding to r_e of 615.6nm.

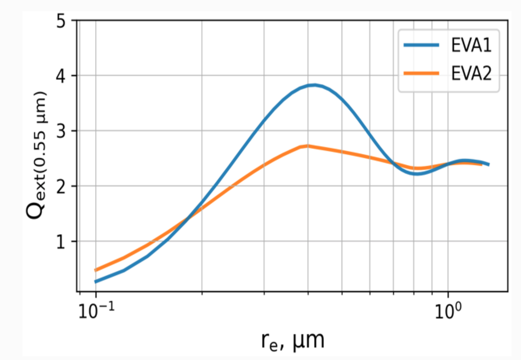

Figure 4: Mie extinction efficiency at 550nm for EVA1 and EVA2.

Single scattering albedo and asymmetry parameter

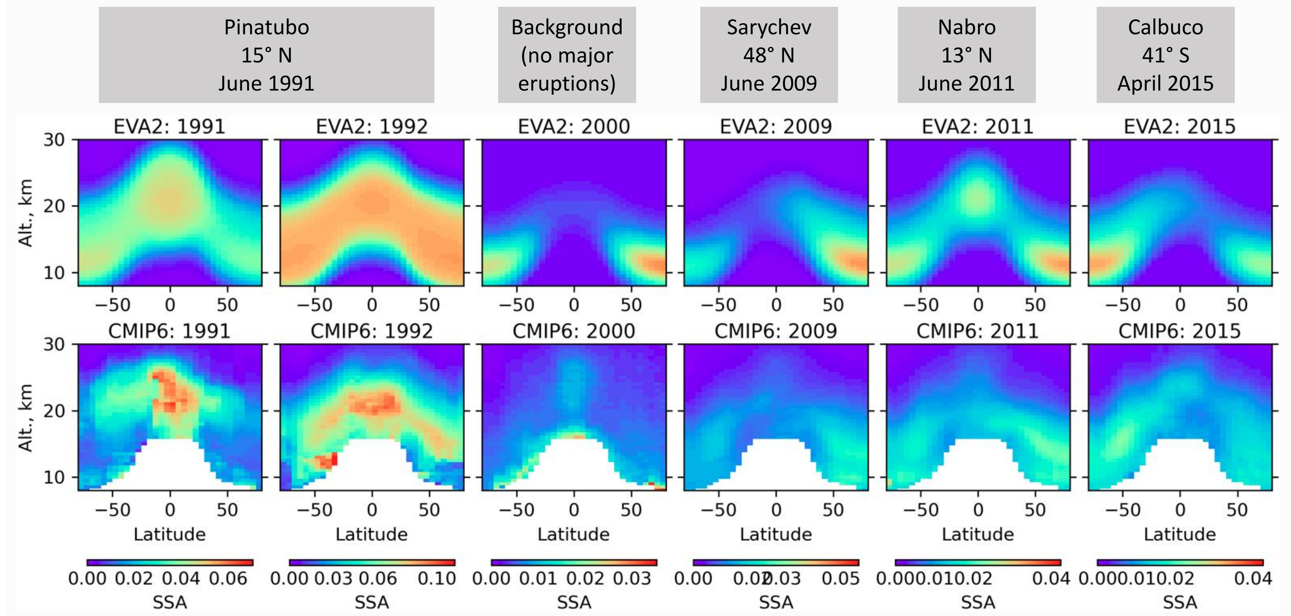

Figure 9: Single Scattering Albedo at 12 µm averaged for selected years. EVA2 output (top) compared to CMIP6 aerosol forcing version 4 dataset (bottom).

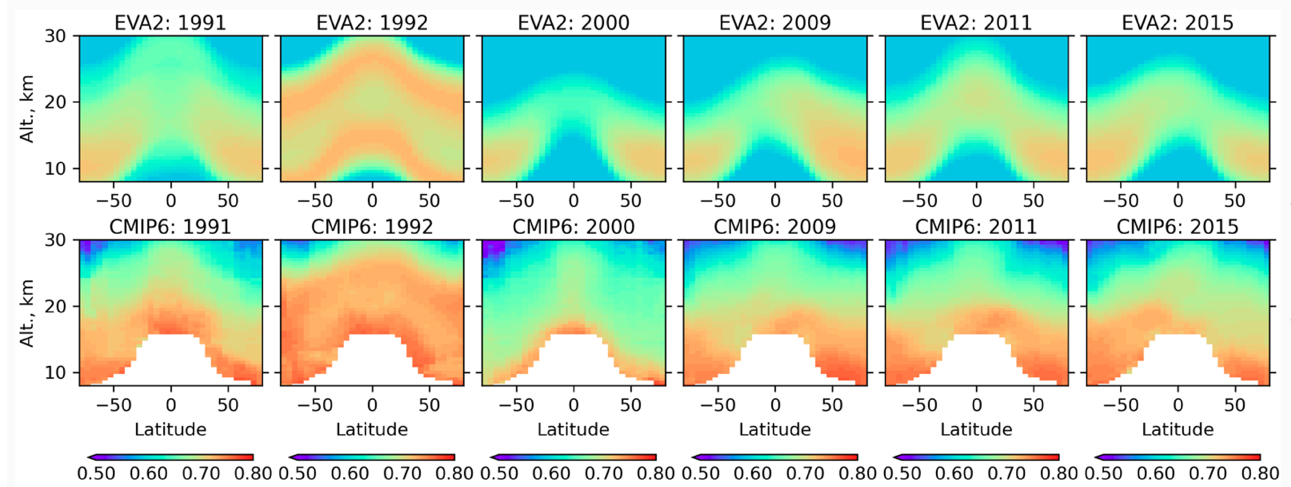

Figure 10: Asymmetry parameter at 550 nm averaged for selected years. EVA2 output (top) compared to CMIP6 aerosol forcing version 4 dataset (bottom).

Aerosol extinction and effective radius

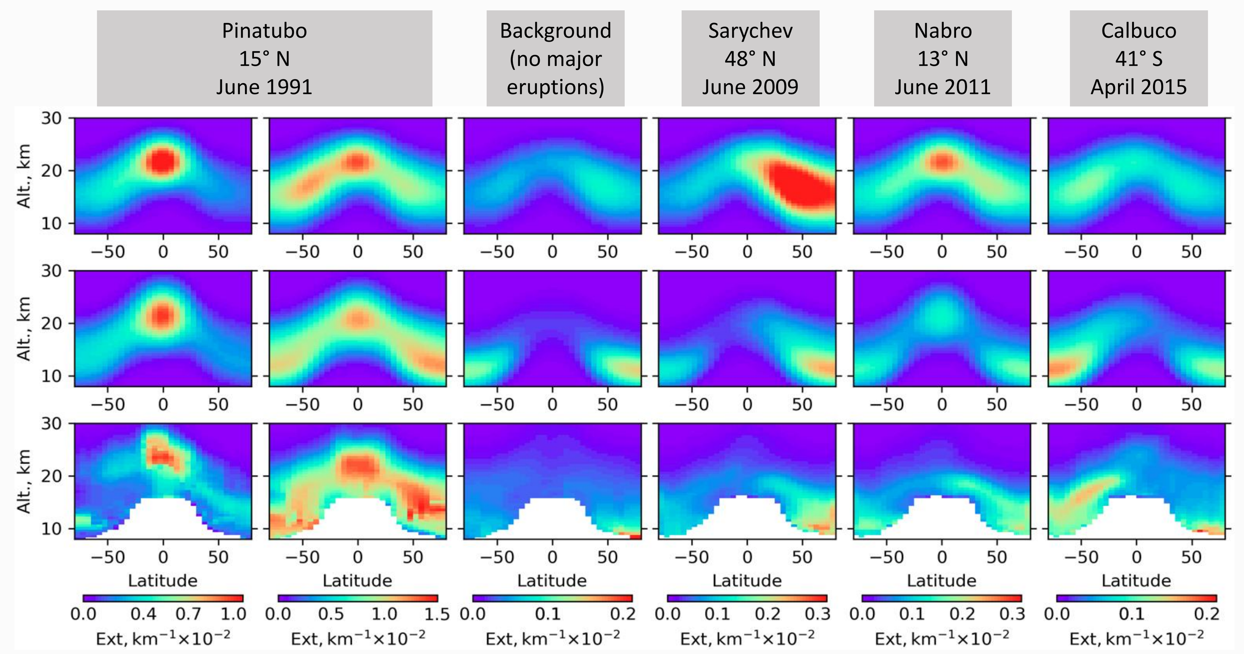

Figure 5: Aerosol extinction coefficient at 525nm averaged for selected years of the satellite era. EVA1 (top) compared to EVA2 (middle) and GloSSAC observations (bottom).

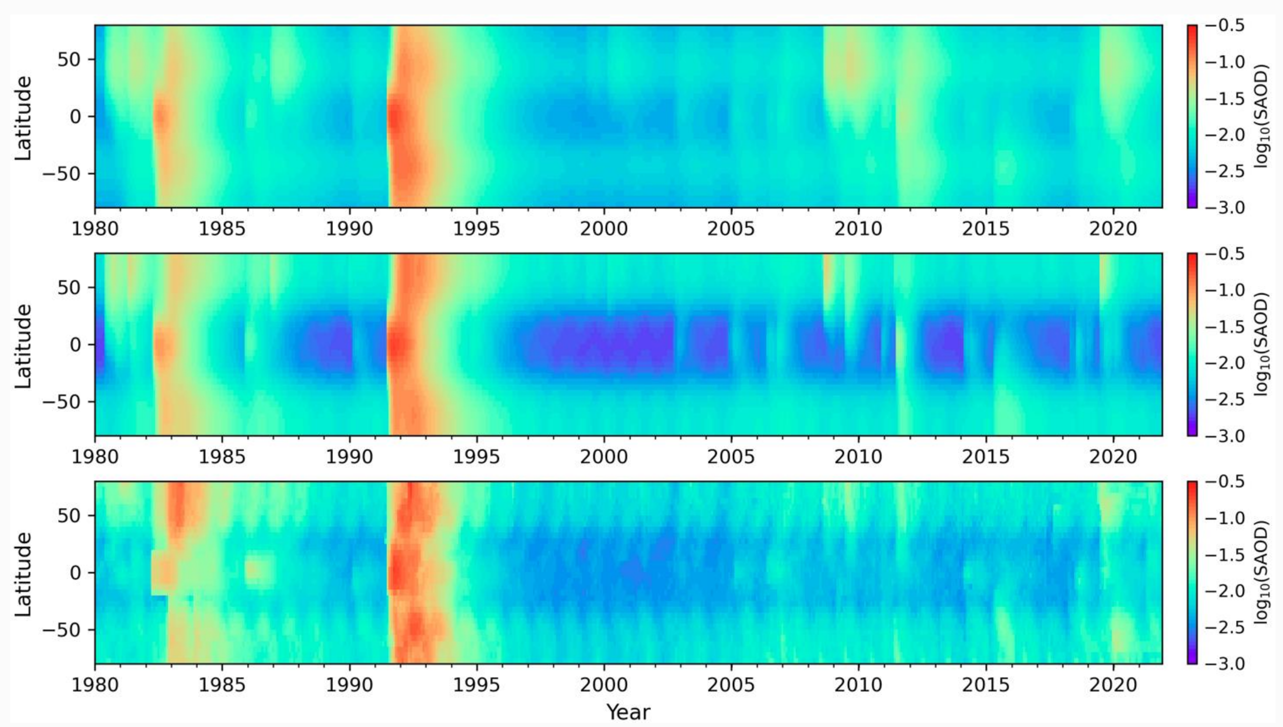

Figure 6: Zonal mean stratospheric aerosol optical depth at 525nm over the satellite era: EVA1 (top) compared to EVA2 (middle) and GloSSAC observations (bottom).

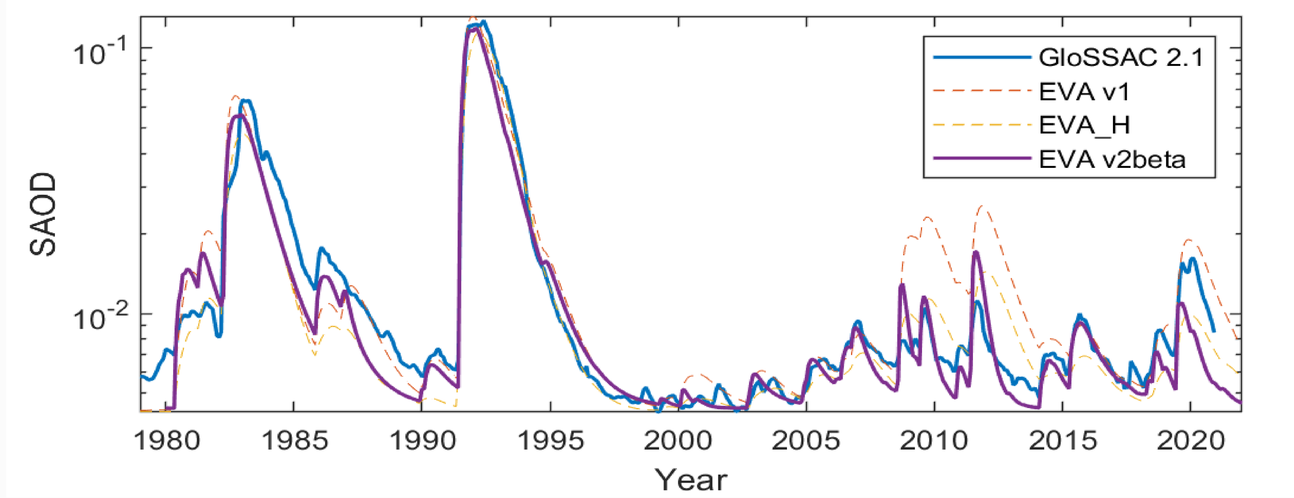

Figure 7: Global mean stratospheric aerosol optical depth (SAOD) over the satellite era: observations from GloSSAC compared to timeseries from EVA1, EVA_H and EVA2.

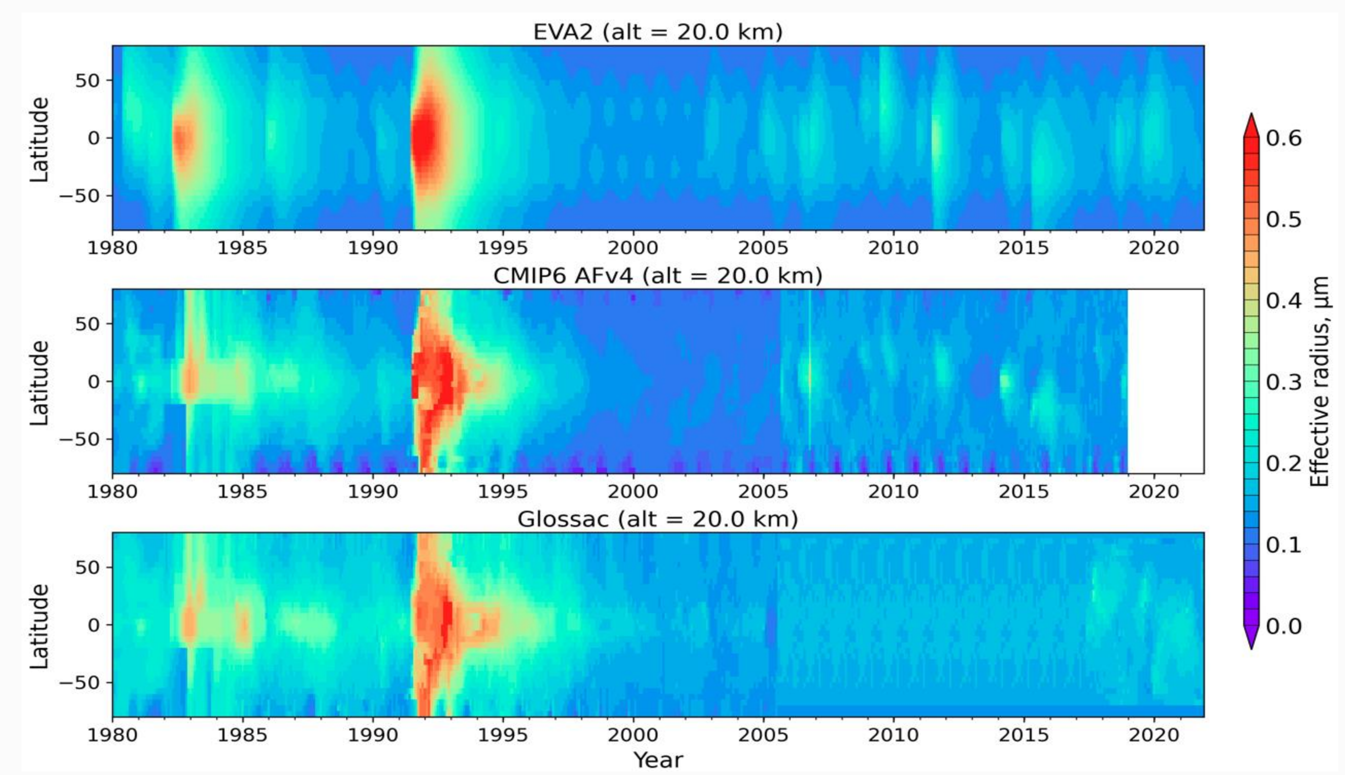

Figure 8: Zonal mean effective radius over the satellite era. EVA2 (top) compared to CMIP6 aerosol forcing version 4 data (middle) and GloSSAC results (bottom). GloSSAC values are derived using 525 and 1020 nm extinction ratio based on Mie scattering calculations, therefore size information is lacking between 2005 and 2017 when multi-wavelength SAGE measurements were not available.

Conclusions and Outlook

- EVA2 shows much improved agreement with satellite aerosol observations with relatively minor increases in complexity
- Other upgrades include:
  - Options for output of physical aerosol properties including surface area density (SAD), number density, volume density, mean radius
  - Ability to specify a time dependent background injection
  - Options for time resolution other than monthly
- Interactive stratospheric aerosol model simulations of very large eruptions will be used as a basis for better representing aerosol forcing for very large eruptions
- To apply EVA2 to the past (beyond the satellite era) we will need estimates of injection height as well as the sulfur injection amount and location. Information from a variety of sources (tephra, ice core isotopes, high temporal resolution cores) will be useful and will need to be integrated!
- EVA2 will be used to provide updates to eVolv2k (Toohey and Sigl, 2017) and HolVol (Sigl et al., 2022), incorporating best estimates of sulfur injection height from the community.

References

Aubry, T. J., Toohey, M., Marshall, L., Schmidt, A. and Jellinek, A. M. (2020): A New Volcanic Stratospheric Sulfate Aerosol Forcing Emulator (EVA_H): Comparison With Interactive Stratospheric Aerosol Models, *J. Geophys. Res. Atmos.*, 125(3).

Biermann, U. M., Luo, B. P., & Peter, T. (2000): Absorption spectra and optical constants of binary and ternary solutions of H2SO4, HNO3, and H2O in the mid infrared at atmospheric temperatures. *J. Phys. Chem. A.*, 104(4), 783–793.

Carn, S. A. (2022): Multi-Satellite Volcanic Sulfur Dioxide L4 Long-Term Global Database V4, Goddard Earth Sci. Data Inf. Serv. Cent. (GES DISC).

Deshler, T., Johnson, B. J., and Rozier, W. R. (1993): Balloonborne measurements of Pinatubo aerosol during 1991 and 1992 at 41∘ N: Vertical profiles, size distribution, and volatility, *Geophys. Res. Lett.*, 20, 1435–1438.

Hummel, J., E. Shettle, and D. Longtin, (1988): A new background stratospheric aerosol model for use in atmospheric radiation models, Tech. Rep. AFGL-TR-88-0166, Air Force Geophys. Lab., Hansom Air Force Base, Mass.

Kovilakam, M., W. Thomason, L., Ernest, N., Rieger, L., Bourassa, A. and Millan, L. (2020): The Global Space-based Stratospheric Aerosol Climatology (version 2.0): 1979-2018, *Earth Syst. Sci. Data*, 12(4), 2607–2634.

Palmer, K. and Williams, D. (1975): Optical Constants of Sulfuric Acid; Application to the Clouds of Venus?, *Appl. Opt*. 14, 208-219.

Plumb, R. A. (1996): A "tropical pipe" model of stratospheric transport, *J. Geophys. Res*., 101(D2), 3957–3972.

Sigl, M., Toohey, M., McConnell, J. R., Cole-Dai, J. and Severi, M. (2022): Volcanic stratospheric sulfur injections and aerosol optical depth during the Holocene (past 11 500 years) from a bipolar ice-core array, *Earth Syst. Sci. Data*, 14(7), 3167–3196.

Sumlin, B.J., Heinson, W.R., Chakrabarty, R.K. (2018): Retrieving the Aerosol Complex Refractive Index using PyMieScatt: A Mie Computational Package with Visualization Capabilities. *J. Quant. Spectros. Rad. Trans*. 2018 (205) 127-134.

Toohey, M., Stevens, B., Schmidt, H. and Timmreck, C. (2016): Easy Volcanic Aerosol (EVA v1.0): an idealized forcing generator for climate simulations, *Geosci. Model Dev*., 9(11), 4049–4070.

Toohey, M. and Sigl, M. (2017): Volcanic stratospheric sulfur injections and aerosol optical depth from 500 BCE to 1900 CE, *Earth Syst. Sci. Data*, 9(2), 809–831.